Report

Current Biology

Soil Salinity Limits Plant Shade Avoidance

Highlights

- Low-level soil salinity inhibits plant shade avoidance
- The effect of salt is dependent upon abscisic acid
- Salt antagonizes the shade-mediated upregulation of brassinosteroid signaling

Authors

Scott Hayes,
Chrysoula K. Pantazopoulou,
Kasper van Gelderen, ...,
Robert C. Schuurink, Christa Testerink,
Ronald Pierik

Correspondence

r.pierik@uu.nl

In Brief

Intensively farmed crops often experience multiple stresses simultaneously. Here, Hayes et al. show that low-level soil salinity suppresses shade avoidance in plants. Through investigation of the mechanisms underlying this trait, they uncover a regulatory pathway that converges at the level of brassinosteroid signaling.

Hayes et al., 2019, Current Biology *29*, 1669–1676
May 20, 2019
https://doi.org/10.1016/j.cub.2019.03.042

CellPress

Current Biology
Report

Soil Salinity Limits Plant Shade Avoidance

Scott Hayes,[1,4] Chrysoula K. Pantazopoulou,[1] Kasper van Gelderen,[1] Emilie Reinen,[1] Adrian Louis Tween,[1] Ashutosh Sharma,[2] Michel de Vries,[3] Salomé Prat,[4] Robert C. Schuurink,[3] Christa Testerink,[5] and Ronald Pierik[1,6,7,*]
[1]Plant Ecophysiology, Institute of Environmental Biology, Utrecht University, Kruytgebouw, Padualaan 8, 3584CH, Utrecht, the Netherlands
[2]School of Biological Sciences, Life Sciences Building, University of Bristol, Bristol BS8 1TQ, UK
[3]Swammerdam Institute for Life Sciences, University of Amsterdam, Science Park 904, 1098XH Amsterdam, the Netherlands
[4]Centro Nacional de Biotecnología, CSIC, Calle Darwin 3, Madrid 28049, Spain
[5]Laboratory of Plant Physiology, Wageningen University and Research, Radix Building, Wageningen 6700 AA, the Netherlands
[6]Twitter: @ronaldpierik
[7]Lead Contact
*Correspondence: r.pierik@uu.nl
https://doi.org/10.1016/j.cub.2019.03.042

SUMMARY

Global food production is set to keep increasing despite a predicted decrease in total arable land [1]. To achieve higher production, denser planting will be required on increasingly degraded soils. When grown in dense stands, crops elongate and raise their leaves in an effort to reach sunlight, a process termed shade avoidance [2]. Shade is perceived by a reduction in the ratio of red (R) to far-red (FR) light and results in the stabilization of a class of transcription factors known as PHYTOCHROME INTERACTING FACTORS (PIFs) [3, 4]. PIFs activate the expression of auxin biosynthesis genes [4, 5] and enhance auxin sensitivity [6], which promotes cell-wall loosening and drives elongation growth. Despite our molecular understanding of shade-induced growth, little is known about how this developmental program is integrated with other environmental factors. Here, we demonstrate that low levels of NaCl in soil strongly impair the ability of plants to respond to shade. This block is dependent upon abscisic acid (ABA) signaling and the canonical ABA signaling pathway. Low R:FR light enhances brassinosteroid (BR) signaling through BRASSINOSTEROID SIGNALING KINASE 5 (BSK5) and leads to the activation of BRI1 EMS SUPPRESSOR 1 (BES1). ABA inhibits BSK5 upregulation and interferes with GSK3-like kinase inactivation by the BR pathway, thus leading to a suppression of BES1:PIF function. By demonstrating a link between light, ABA-, and BR-signaling pathways, this study provides an important step forward in our understanding of how multiple environmental cues are integrated into plant development.

RESULTS AND DISCUSSION

Soil Salinity Inhibits Plant Shade Avoidance

Soil salinity is detrimental to plants and often results in a reduction in stem and root biomass accumulation [7]. Most previous studies have, however, focused on the effects of salt at a range of very high concentrations (at a median concentration of 150 mM NaCl) [8]. We opted for a nuanced approach to investigate how low concentrations of NaCl may affect plant shade avoidance. Growing plants in tissue culture often masks genes involved in NaCl sensitivity [9, 10], and so for phenotypic experiments plants were grown on soil. *Arabidopsis thaliana* (*Arabidopsis*) seeds were germinated under white light (Wl) for 3 days, before transfer to new soil that had been pre-treated with NaCl solution. Following this, plants were returned to Wl for a further day to acclimate, before they were shifted to Wl or Wl with supplementary far-red LEDs (+FR). Hypocotyl lengths were measured on day 7 (for a schematic diagram of the treatments see Figure S1A). Water or NaCl solution was applied from below, and the soil was kept saturated to avoid dehydration.

We observed a strong NaCl-mediated reduction in +FR-induced hypocotyl elongation when plants were watered with as low as 10 mM NaCl (Figure 1A). Increasing NaCl concentrations beyond 25–75 mM NaCl provided no further inhibition of +FR-induced hypocotyl elongation, and so 25 mM NaCl was selected for further investigation. NaCl inhibited +FR-induced elongation across the 3 days of +FR treatment (Figure S1B). In adult plants, 25 mM NaCl exerted a strong inhibition of +FR-induced rosette expansion, mostly through an inhibition of lamina elongation (Figures 1B, 1C, S1C, and S1D). Additionally, we found that NaCl inhibited +FR-induced elongation in tomato and tobacco seedlings (Figures 1D and 1E), raising the possibility that this is a general phenomenon in shade-avoiding plants.

Soil Salinity Acts through the ABA Pathway

Many plant responses to soil salinity are mediated through the hormone abscisic acid (ABA) [11]. We found that transcripts of *SAG29* (an ABA-responsive gene [12]) accumulated to high levels in +NaCl +FR conditions (Figure 2A). This accumulation did not occur in plants lacking four ABA-responsive transcription factors (*ABA-responsive element-binding factor 1*, *2*, *3*, and *4* [13], here referred to as *arebQ*). We therefore decided to assess whether ABA signaling is required for NaCl-mediated inhibition of +FR-induced elongation. In mutants that lacked either four of the ABA receptors (*pyr1/pyl1/pyl2/pyl4*- here referred to as *abaQ* [14]) or two ABA-signaling kinases (*sucrose non-fermenting 1-related protein kinase 2.2* and *2.3*- *snrk2.2snrk2.3*) [15],

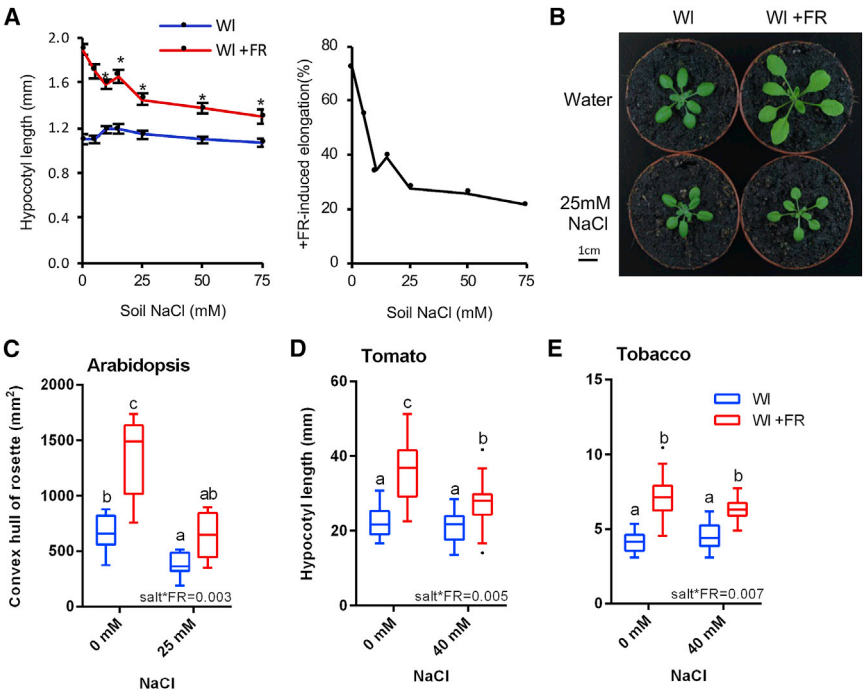

Figure 1. Soil Salinity Inhibits +FR-Induced Elongation

(A) Left: hypocotyl length of 7-day-old Col seedlings germinated in WI, transferred to NaCl soil of the indicated concentration at day 3, and then shifted to WL ± FR at day 4. Data represent mean ($n \geq 19$) ±SE. Asterisks indicate salt-mediated inhibition of hypocotyl elongation compared to 0 mM NaCl control; Student's t test ($p < 0.05$). Right: the same data expressed as the percentage of +FR-induced elongation at each salt concentration.

(B) Representative 21-day-old Col plants germinated in WI and transferred to ±25 mM NaCl at day 3, before shifting to WL ± FR at day 10.

(C) Rosette circumference of plants grown as in (B) ($n \geq 10$).

(D) Hypocotyl length of 11-day-old tomato (*Solanum lycopersicum* var. "Moneymaker") seedlings germinated in WI, transferred to ±40 mM NaCl at day 7, and shifted into WL ± FR at day 8 ($n \geq 19$).

(E) Hypocotyl length of tobacco (*Nicotiana benthamiana*) seedlings grown as in (D) ($n \geq 18$). Boxplots are visualized by the Tukey method. In all figures, different letters designate significantly different means by 2-way ANOVA + Tukey's post hoc test ($p < 0.05$). Interaction p value is shown inset.

See also Figure S1.

NaCl no longer had an effect on +FR-induced hypocotyl elongation (Figures 2B and 2C). Whereas plants lacking a single ABA activated transcription factor, *ABA INSENSITIVE 5* (*abi5-1*), still showed a strong NaCl-mediated inhibition of hypocotyl elongation under +FR light (Figure S2A), plants lacking the *AREB* quartet (*arebQ*) elongated to the same extent in the presence and absence of NaCl (Figure 2D). Taken together, these results suggest that the effect of NaCl on +FR-induced elongation is dependent upon enhanced ABA synthesis or signaling.

In addition to these mutant and gene expression analyses, we found that applying increasing concentrations of ABA directly between the cotyledons had a similar effect as applying increasing NaCl concentrations to the soil (Figure 1A versus Figures S2B). Low concentrations of ABA provided a strong break on hypocotyl elongation in +FR light; this inhibition was saturated by 10 μM ABA and remained constant until at least 100 μM ABA. As with NaCl, the inhibition of +FR-induced hypocotyl elongation by exogenous ABA was absent in the *abaQ* (Figure S2C) and *snrk2.2/snrk2.3* mutants (Figure S2D). Despite the clear requirement for ABA signaling, NaCl still inhibited +FR-induced elongation in mutants that have reduced levels of ABA synthesis, such as *aba2-1* and *aba3-1* (Figures S2E and S2F), and we were unable to detect any increase in ABA levels in whole NaCl-grown seedlings (Figure S2G). It may be that ABA signaling is enhanced only locally, ABA distribution is altered, or that there is direct activation of the ABA signal pathway by an unknown mechanism.

Salt and ABA Impede upon PIF4/PIF5 Action

We next investigated the manner in which ABA and NaCl inhibit +FR-induced elongation. The induction of hypocotyl elongation by +FR requires PIF4, PIF5, and PIF7 [3, 4, 16] (Figure 3A). In our conditions, PIF7 was the dominant PIF driving +FR-induced hypocotyl elongation, as the *pif7* single mutant showed no significant +FR-induced elongation and there were no additional effects in the *pif4/pif5/pif7* triple mutant. Single *pif4* or *pif5* mutants appeared similar to the wild-type, with strong +FR-induced hypocotyl elongation that was inhibited by NaCl. The *pif4/pif5* double mutant did however show reduced +FR-induced elongation, suggesting that these genes act redundantly. Notably, the hypocotyl length of the *pif4/pif5* mutant in +FR light was the same as NaCl +FR-treated wild-type plants, and NaCl did not further suppress elongation in this mutant (Figure 3A). In a similar fashion to NaCl, ABA inhibited +FR-induced hypocotyl elongation in the wild-type to the same length as the *pif4/pif5* mutant, and ABA had no further effect on elongation in this mutant (Figure S2C). These findings suggest that NaCl and ABA could act to suppress PIF4/PIF5 function.

We found that the expression of two +FR-induced genes (*PRE1* and *SAUR16*) was suppressed by pre-treatment with NaCl. In the *pif4/pif5* mutant, however, NaCl did not affect the expression of these genes (Figure S3A). We used plants expressing luciferase (LUC) reporter constructs to investigate salt-mediated inhibition of +FR-induced genes over a longer timescale. When LUC expression was driven by the *PIL1* [17] or *IAA19* promoter, +FR light resulted in a rapid induction of LUC activity, and NaCl and ABA caused a sustained suppression of this upregulation over several days (Figure S3B). As both the *PIL1* and *IAA19* promoters contain several G-boxes (Figure S3C) that are established PIF4 and PIF5 direct targets [5, 18], these results are consistent with NaCl and ABA-mediated inhibition of PIF4 and PIF5 activity.

PIFs promote hypocotyl elongation in +FR light through an increase in auxin signaling [2]. To investigate whether NaCl and

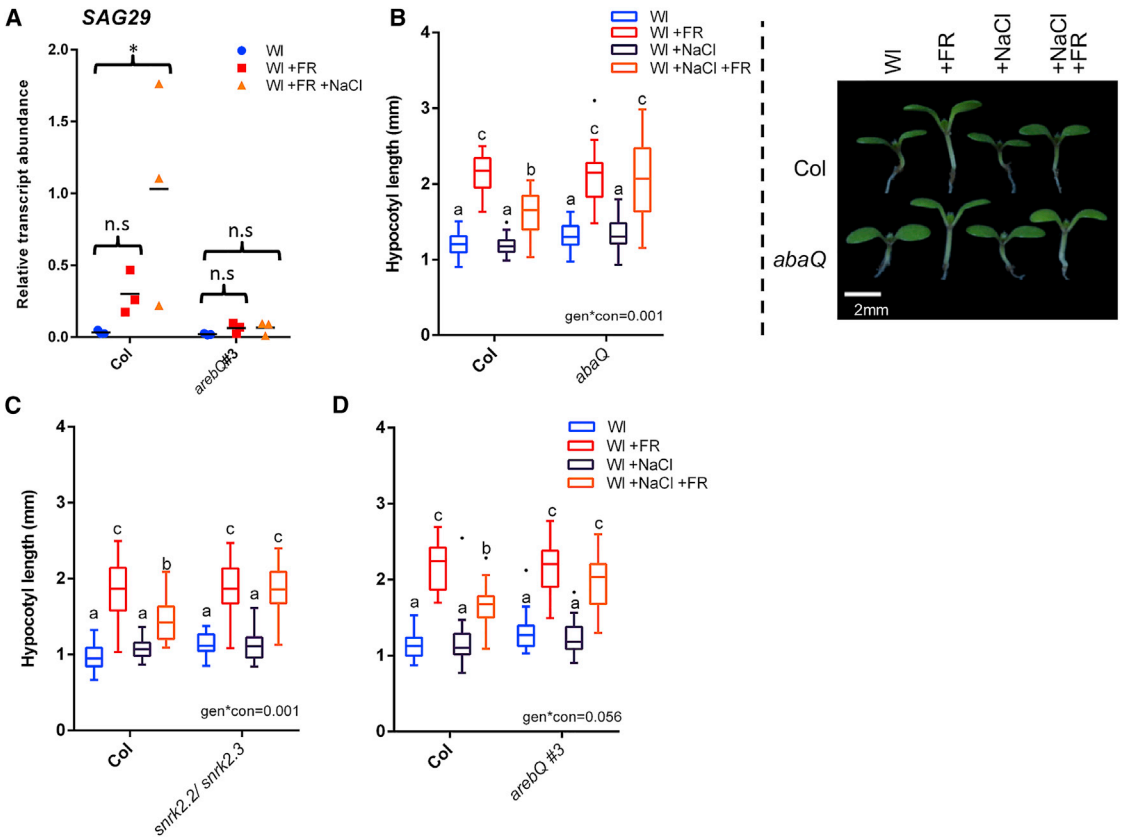

Figure 2. Salinity-Mediated Inhibition of +FR-Induced Elongation Requires ABA Signaling

(A) Relative *SAG29* transcript abundance in the hypocotyls of Col and *arebQ* mutant plants grown 3 days in WI, transferred to ±25 mM NaCl soil at day 3, and then shifted to WL ± FR at day 4. Tissues were harvested at Zeitgeber time (ZT) 4.5 on day 6 (n = 3). *Significant difference from WI control.

(B–D) Hypocotyl lengths of 7-day-old wild-type and (B) *abaQ*, (C) *snrk2.2*/snrk2.3, and (D) *arebQ* mutants germinated in WI, transferred to ±25 mM NaCl soil at day 3, and then shifted to WL ± FR at day 4 (n ≥ 22).

Right image of (A) depicts representative seedlings grown in these conditions. Boxplots are visualized by the Tukey method. Gene expression studies show individual values, with a horizontal bar representing the mean. Different letters designate significantly different means by 2-way ANOVA + Tukey's post hoc test ($p < 0.05$). Interaction p value is shown inset.

See also Figure S2 and STAR Methods.

ABA suppressed auxin signaling, we generated a *DR5v2:GUS* (β-glucuronidase) auxin reporter line. *DR5v2* is a synthetic promoter that was developed as a more sensitive auxin reporter than the widely used *DR5* [19]. Three independent *DR5v2:GUS* lines were tested and confirmed to be highly auxin responsive (Figure S3D). We found that, when grown under supplementary FR light, *DR5v2:GUS* plants had increased GUS staining at the upper part of the hypocotyl, but that this response was attenuated in the presence of NaCl (Figures 3B and S3E). We then crossed this line into the *pif4/pif5* mutant background. In the absence of *PIF4* and *PIF5*, we no longer detected a +FR-mediated increase in GUS staining, and salt had no further effect on this mutant (Figures 3B and S3E). Again, this is consistent with an NaCl-mediated inhibition of PIF4/ PIF5 activity.

In wild-type plants, auxin application promoted hypocotyl elongation in all of our growth conditions, but NaCl still significantly inhibited +FR-induced elongation in the presence of supplementary auxin (Figure S3F), suggesting that NaCl may act to suppress auxin sensitivity or transport [20]. Supplementary auxin also enhanced hypocotyl elongation in the *pif4/pif5* mutant in most of the conditions tested but did not rescue elongation in this mutant to the same length as wild-type plants treated with auxin and +FR (Figure S3F). NaCl had no effect on +FR-induced elongation in the *pif4/pif5* mutant, even in the presence of supplementary auxin, which is in accordance with the role of PIF4 and PIF5 in the control of auxin signaling [6].

PIFs are often regulated by light at the level of protein stability [3, 21], so we assessed the abundance of constitutively expressed PIF4-HA and PIF5-HA under +FR and +NaCl conditions. While 2-way ANOVAs revealed an effect of NaCl on PIF4 stability, we did not see a statistically significant reduction in PIF4 protein levels in any of the individual light conditions tested (Figure 3C). PIF5 was stabilized by +FR light, but NaCl had no significant effect on this stabilization (Figure 3C). Additionally, we observed no changes in *PIF4* or *PIF5* expression in NaCl or in the *arebQ* mutant (Figure 3D).

Brassinosteroid Pathway Is Inhibited by Salt and ABA

We hypothesized that PIF4 and PIF5 action could be inhibited through a change in activity of one of their interaction partners.

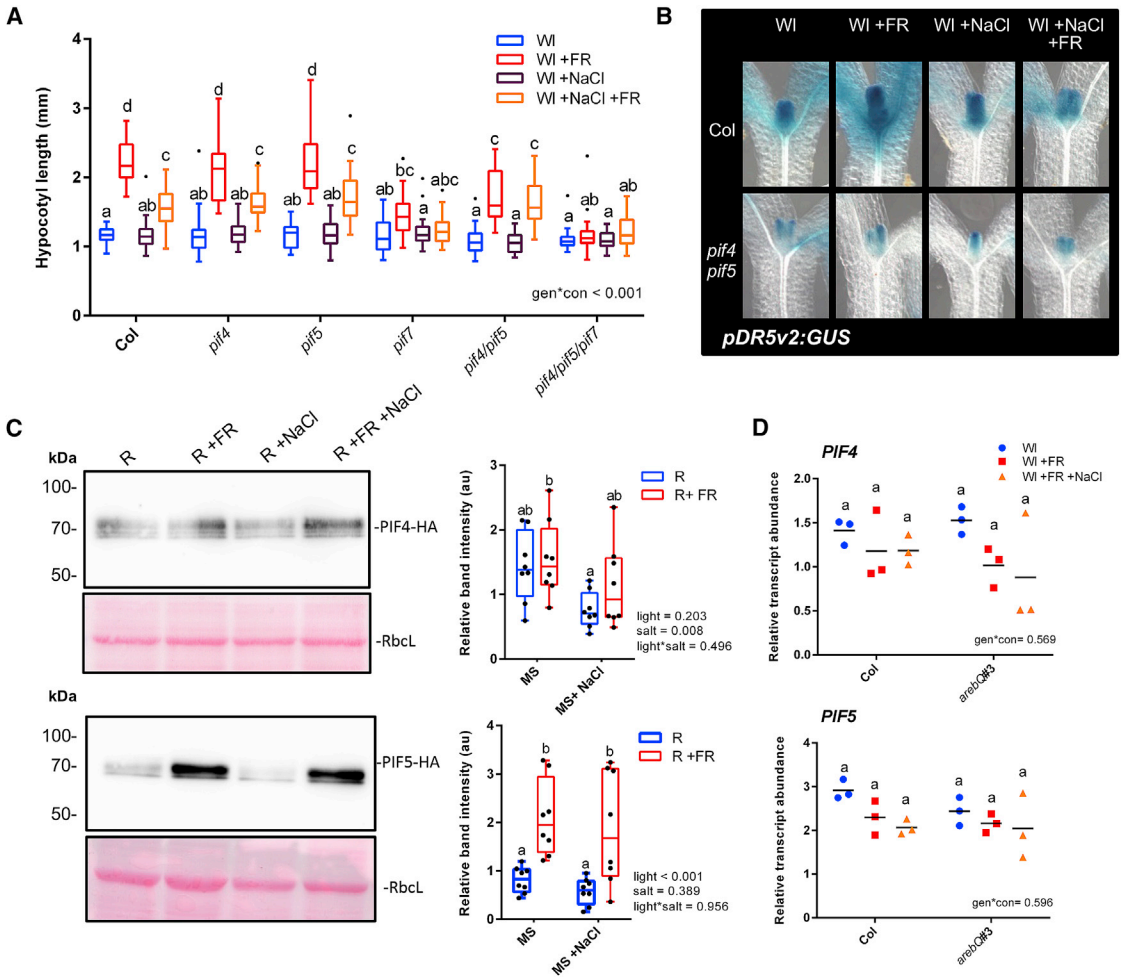

Figure 3. Soil Salinity Suppresses PIF Function and +FR-Induced Gene Expression and Auxin Signaling

(A) Hypocotyl length of 7-day-old Col, *pif4-101*, *pif5*, and *pif7-1* double- and triple-mutant seedlings germinated in WI, transferred to 25 mM NaCl soil at day 3, and then shifted to WL ± FR at day 4 ($n \geq 23$).

(B) Seedlings expressing a *pDR5v2:GUS* reporter in the Col or *pif4-101/pif5* background were germinated in WI and transferred to ±25 mM NaCl soil on day 3. On day 4 at plants were shifted to WL ± FR and seedlings were fixed on day 5 at ZT 4.5. Representative hypocotyls of GUS stained seedlings are shown (quantification of the top half of the hypocotyls is shown in Figure S3E).

(C) Western blots of *35S:PIF4-HA* (top) and *35S:PIF5-HA* (bottom) plants germinated on plates in WI, transferred to 75 mM NaCl plates, and grown for a further 2 days in R light. At ZT 3 on day 5, plants were moved to R ± FR for 1 h, and seedlings were harvested into liquid N_2. Western blots probed with anti-HA. Pink lanes show Ponceau staining of rubisco large subunit (RbcL) as a loading control. The right image depicts relative band intensity after normalization to RbcL (n = 8, across 4 separate experiments).

(D) Relative *PIF4* (top) and *PIF5* (bottom) transcript abundance in the hypocotyls of Col and *arebQ* mutant plants grown as in (A) that were harvested at ZT 4.5 on day 6 (n = 3).

Boxplots are visualized by the Tukey method (if $n \geq 10$) or as max-min with every value shown (if $n < 10$). Gene expression studies show individual values, with a horizontal bar representing the mean. In all figures, different letters designate significantly different means by 2-way ANOVA + Tukey's post hoc test ($p < 0.05$). See also Figure S3 and STAR Methods.

PIF action is suppressed by competitive heterodimerization with DELLA proteins [22, 23]. It has previously been shown that NaCl stabilizes DELLA proteins [24] and DELLA degradation is required for +FR-induced shade avoidance to occur [25]. Mutants lacking all five DELLA proteins showed longer hypocotyls than the wild-type in all of our conditions (Figure S4A) but still exhibited a strong NaCl-mediated inhibition of +FR-induced elongation. This suggests that NaCl inhibits shade avoidance through another mechanism. A recent study found that the stabilization of DELLAs by NaCl in the root is transient [26], and so it may be that their role is restricted to growth arrest upon initial NaCl exposure.

In NaCl-treated roots, ABA production precedes a reduction of BR signaling [26] and it is known that BR signaling is necessary for +FR-induced hypocotyl elongation to occur [16]. This raises the possibility that during NaCl exposure ABA acts to inhibit BR signals. We tested the effect of brassinazole (BRZ- an inhibitor of BR synthesis) on hypocotyl elongation under +FR light. We found that BRZ, much like both NaCl and ABA, inhibited hypocotyl elongation very readily at low concentrations and that this

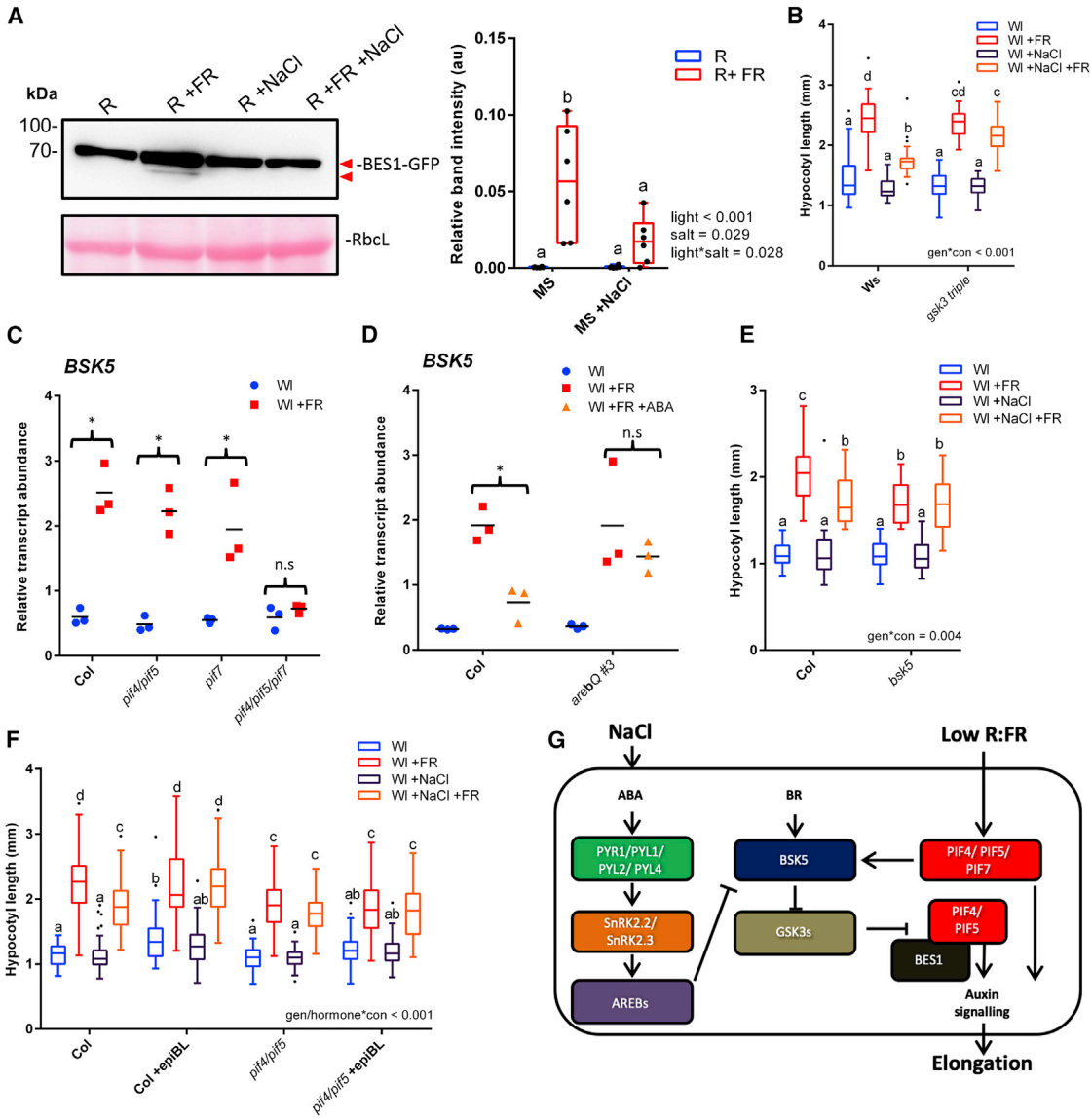

Figure 4. ABA and NaCl Inhibit +FR Elongation through Inhibiting BR Signaling

(A) *35S:BES1-GFP*-expressing plants were germinated on plates for 3 days in WI, transferred to ±75 mM NaCl plates, and then grown in R light for 2 further days. On day 5, plants were shifted to R ± FR at ZT 3 and tissue was harvested at ZT 4. Proteins were identified through western blots with anti-GFP. Right image shows quantified lower band intensity relative to RbcL (n = 6).

(B) Hypocotyl length of 7-day-old Wassilevskija (Ws) and *gsk3-triple* mutant germinated in WI, transferred to ±25 mM NaCl soil at day 3, and then shifted to WL ± FR at day 4 ($n \geq 24$).

(C) Col and *pif4-101/pif5*, *pif7-1*, and *pif4-101/pif5/pif7-1* plants were germinated in WI for 3 days before transfer to new pots. At ZT 2.5 on day 7, plants were shifted to WI ± FR light. At ZT 4.5, the hypocotyls of approximately 20 seedlings per sample were dissected and RNA was extracted. *BSK5* transcripts relative to *AT1613320* are shown (n = 3). *+FR-induced increase.

(D) Col and *arebQ #3* plants were grown as in (C). At ZT 1.5 on day 7, plants were sprayed with 25 μM ABA and exposed to WI ± FR at ZT 2.5. At ZT 4.5, the hypocotyls of approximately 20 seedlings per sample were dissected and RNA extracted. *BSK5* transcripts relative to *AT1613320* are shown (n = 3). *ABA-mediated decrease.

(E) Hypocotyl length of Col and *bsk5* grown as in (B) ($n \geq 22$).

(F) Hypocotyl length of 7-day-old Col and *pif4-101/pif5* plants grown as in (B), with applications 10 μM epi-BL or ethanol control on days 3–6 ($n \geq 46$).

(G) A proposed mechanism for salt-mediated inhibition of low R:FR-induced elongation. Low R:FR light promotes the stability of PIF4, 5 and 7. These PIFs redundantly upregulate the expression of *BSK5*. BSK5 acts to suppress the activity of GSK3-like kinases, which relieves their suppression of the PIF:BES1 signaling module in a positive feedback loop. NaCl promotes the canonical ABA signal transduction pathway, resulting in the increased activity of AREB transcription factors. AREBs inhibit the upregulation of *BSK5* and thereby enhance GSK3-like kinase action. GSK3-like kinases are then free to inhibit the PIF:BES1 signaling module, limiting auxin signaling in the hypocotyl.

(legend continued on next page)

inhibition remained constant as concentrations increased (Figure S4B). Intriguingly, hypocotyl length at this plateau was equal to that of +FR-treated plants grown on saline soil in the absence of BRZ. Furthermore, simultaneous application of ABA, BRZ, and NaCl had no further effect on the hypocotyl length of +FR-treated plants than NaCl treatment alone (Figure S4C), consistent with these compounds converging on the same pathway. Supporting this, application of epi-brassinolide (BL) rescued +FR-induced hypocotyl elongation in NaCl-exposed plants (Figure S4D). Hypocotyl length was rescued at low concentrations of epi-BL, up to the extent of +FR-treated control plants grown in the absence of NaCl (Figure S4D). We also observed that epi-BL could not rescue hypocotyl elongation in the *yucca2589* mutant (Figure S4E), which probably indicates that in our conditions, BR-mediated rescue of hypocotyl elongation is auxin dependent.

Although it is known that inhibition of BR signaling inhibits shade avoidance, it is currently unclear whether +FR enhances BR signals. We assessed BR activity through looking at BES1 phosphorylation levels in a *35S:BES1-GFP* line. We found that short-term +FR treatments rapidly resulted in a faster running form of BES1 (Figure 4A), which has previously been shown to correspond to the active, de-phosphorylated form of the protein [27]. We found that NaCl inhibited the +FR-mediated induction of this faster running band (Figure 4A), suggesting that BES1 activation by +FR light is inhibited by NaCl. Despite this, we found that plants that hyper-accumulate BES1 (*bes1-D* mutants) actually had shorter hypocotyls under +FR than wild-type plants (Figure S4F). Recently, it has been shown that the balance between BES1 and PIF4 levels dictates whether BES1 acts as an activator or repressor of BR synthesis genes [28]. Over-accumulation of BES1 suppresses BR synthesis genes and, since PIF4 activity is directly suppressed in the absence of BR [29], this may explain the reduced +FR response in the *bes1-D* line.

BES1 phosphorylation is mediated through BRASSINOSTEROID INSENSITIVE 2 (BIN2- a GSK3-like kinase), which acts as a negative regulator of the BR pathway. Previously, it was shown that ABA enhances the kinase activity of BIN2 toward BES1 [30]. We found that mutants that lack BIN2 and two closely related GSK3 kinases (*gsk3 triple*) no longer showed inhibition of +FR-induced elongation in response to NaCl, ABA, or BRZ (Figures 4B and S4G).

ABA Inhibits +FR-Induced Expression of BSK5

We reasoned that the inhibition of GSK3 kinase function may be required for full +FR-induced hypocotyl elongation. Upstream of GSK3 kinases in the BR signal cascade are the BRASSINOSTEROID SIGNALING KINASES (BSKs). BSK activation by BR [31] results in the inactivation of GSK3 kinases [31–33]. Despite high redundancy between the 12 BSK family members [33], mutation of just one (*BSK5*) alters plant sensitivity to NaCl and ABA [34]. Interestingly, *BSK5* transcripts are enhanced in hypocotyls under +FR light [35]. We found that this upregulation was redundantly regulated by *PIF4*, *PIF5*, and *PIF7* (Figure 4C).

The *BSK5* promoter contains a G-box approximately 3.5 kb from its start codon (Figure S4H). Multiple PIFs bind directly to this G-box [18], as does at least one AREB family member, ABF3 (in an ABA-dependent manner) [12]. We found that ABA pre-treatment strongly inhibited the +FR-mediated upregulation of *BSK5* transcripts in hypocotyls (Figure 4D) and that ABA-mediated repression of *BSK5* transcripts was dependent upon AREB family transcription factors. +FR-induced hypocotyl elongation was dependent upon *BSK5* as *bsk5* mutants showed only limited +FR-induced elongation (Figure 4E). This elongation was to a similar length as wild-type plants treated with +FR and NaCl, and NaCl had no further effects on +FR-induced elongation in a *bsk5* mutant (Figure 4E). These results demonstrate that the +FR-mediated upregulation of *BSK5* is required for maximal hypocotyl elongation under +FR light, and they suggest that ABA may at least in part inhibit +FR-induced elongation through a suppression of *BSK5* transcription.

Repression of +FR-Induced Elongation Centers on the PIF-BES1 Module

Importantly, the rescue of hypocotyl elongation by epi-BL did not occur in the *pif4*/*pif5* mutant, demonstrating that in this context, BR-induced growth requires *PIF4* and/or *PIF5* (Figure 4F). Recent reports have demonstrated a close regulatory relationship between PIF and brassinosteroid signaling. Brassinosteroid upregulates each of the shade-induced genes that we tested (*PIL1*, *IAA19*, *SAUR16*, and *PRE1*) [29, 36, 37]. PIF4 heterodimerizes with BES1 [28] and a BES1 homolog, BRASINAZOLE RESISTANT 1 (BZR1), and inter-dependently they control the expression of thousands of genes [38]. Additionally, BIN2 has a direct inhibitory effect on both PIF4 [29] and PIF3 [39].

From our results, we propose a mechanism (Figure 4G) whereby +FR light promotes the activity of PIF4, PIF5, and PIF7, and these transcription factors then redundantly promote the expression of *BSK5*. BSK5 suppresses GSK3-like kinases, allowing for the activation of the BES1:PIF4/PIF5 signaling module. In saline soils, activation of the ABA signal transduction pathway results in the enhanced action of AREB/ABF transcription factors that suppress *BSK5* transcription, and therefore break the +FR-induced PIF:BES1 feedforward loop. The absence of BSK5 would allow for strong GSK3-like kinase action, leading to a suppression of the BES1:PIF4/PIF5 signal module. We do not rule out other mechanisms by which NaCl may inhibit +FR-induced elongation; indeed, we found that mutants lacking the evening complex component *ELF3* had elongated hypocotyls in all of our growth conditions and appeared to lack NaCl-mediated inhibition of +FR-induced hypocotyl elongation (Figure S4H). This implies that NaCl may also suppress PIF4 and PIF5 through the circadian clock.

There may be an adaptive significance to our finding that plants grown in saline soils suppress BES1:PIF signaling when they are presented with shade cues. Indeed, a recent study suggested that overexpression of *PIF4* may reduce plant survival in

Boxplots are visualized by the Tukey method (if $n \geq 10$) or as max-min with every value shown (if $n < 10$). Gene expression studies show individual values, with a horizontal bar representing the mean. Where letters are shown, different letters designate significantly different means by 2-way ANOVA + Tukey's post hoc test ($p < 0.05$).
See also Figure S4 and STAR Methods.

saline conditions [40]. It is possible then that shade avoidance signaling is detrimental to salt survival. It is notable that BR-based chemicals are currently being developed as treatments for salt and drought afflicted crops [41]. It may be that, under concurrent salt and shade conditions, re-activation of the BR signal cascade is damaging to plant health.

STAR★METHODS

Detailed methods are provided in the online version of this paper and include the following:

- KEY RESOURCES TABLE
- CONTACT FOR REAGENT AND RESOURCE SHARING
- EXPERIMENTAL MODEL AND SUBJECT DETAILS
- PLANT PROPAGATION
- METHOD DETAILS
  - Morphological studies
  - Development of Transgenic Lines
  - Gene Expression Studies
  - Luciferase Assay
  - ABA Extraction and Quantification
  - Western Blots
  - GUS Staining
- QUANTIFICATION AND STATISTICAL ANALYSES
  - Image quantification
  - Data presentation
  - Statistical Analyses
- DATA AVAILABILITY

SUPPLEMENTAL INFORMATION

Supplemental Information can be found online at https://doi.org/10.1016/j.cub.2019.03.042.

ACKNOWLEDGMENTS

We would like to thank Prof. Dolf Weijers (WUR, Wageningen, NL) for providing the *pUC57:DR5v2* plasmid, Prof. Christian Fankhauser (UNIL, Lausanne, CH) for the *pCF402* and *pCF404* plasmids, Prof. Kazuko Yamaguchi-Shinozaki (The University of Tokyo, Tokyo, Japan) for *arebQ* seeds, Prof. Keara Franklin (The University of Bristol) for the *p35S:PIF4-HA* and *p35S:PIF5-HA* seeds ahead of publication, the Plant Ecophysiology Group (Utrecht University, Utrecht, NL) for help with harvesting and gene expression studies, and Dr. Charlotte Gommers (WUR, Wageningen, NL) for critical reading of this manuscript. S.H. was supported through a fellowship from the European Molecular Biology Organisation (EMBO- ATFL 404-2015) and Marie Skłodowska Curie Actions (792624). The research was funded through the Netherlands Organisation for Scientific Research (NWO, awarded to R.P., VIDI-864.12.003), the Spanish Ministry of Economy and Competitiveness (MINECO, awarded to S.P., BIO2017-90056-R), and the UK Biotechnology and Biological Sciences Research Council (BBSRC, grant BB/M008711/1 to support A.S.). ORCIDs for the authors are as follows: 0000-0001-8943-6238 (S.H.), 0000-0001-5412-6029 (C.K.P.), 0000-0001-7809-2812 (K.v.G.), 0000-0003-0299-7900 (A.L.T.) 0000-0002-9137-0888 (A.S.), 0000-0001-6451-5968 (M.d.V.), 0000-0003-2684-5485 (S.P.), 0000-0002-9223-9996 (R.C.S.), 0000-0001-6738-115X (C.T.), and 0000-0002-5320-6817 (R.P.).

AUTHOR CONTRIBUTIONS

Conceptualization, S.H., C.T., and R.P.; Methodology, S.H., A.L.T., S.P., and R.P.; Formal Analysis, S.H.; Investigation, S.H., C.K.P., K.v.G., A.L.T., E.R., A.S., M.d.V., and S.P.; Resources, S.P., R.C.S., and R.P.; Writing – Original, S.H.; Writing – Review & Editing, S.H., C.K.P., K.v.G., C.T., S.P., R.C.S., and R.P.; Visualization, S.H.; Funding Acquisition, S.H., R.P., and S.P.

DECLARATION OF INTERESTS

The authors declare no competing interests.

Received: March 20, 2018
Revised: December 13, 2018
Accepted: March 20, 2019
Published: May 2, 2019

REFERENCES

1. Ausubel, J.H.J., Wernick, I.K.I., and Waggoner, P.E.P. (2013). Peak Farmland and the Prospect for Land Sparing. Popul. Dev. Rev. *38*, 221–242.
2. Fraser, D.P., Hayes, S., and Franklin, K.A. (2016). Photoreceptor crosstalk in shade avoidance. Curr. Opin. Plant Biol. *33*, 1–7.
3. Lorrain, S., Allen, T., Duek, P.D., Whitelam, G.C., and Fankhauser, C. (2008). Phytochrome-mediated inhibition of shade avoidance involves degradation of growth-promoting bHLH transcription factors. Plant J. *53*, 312–323.
4. Li, L., Ljung, K., Breton, G., Schmitz, R.J., Pruneda-Paz, J., Cowing-Zitron, C., Cole, B.J., Ivans, L.J., Pedmale, U.V., Jung, H.S., et al. (2012). Linking photoreceptor excitation to changes in plant architecture. Genes Dev. *26*, 785–790.
5. Hornitschek, P., Kohnen, M.V., Lorrain, S., Rougemont, J., Ljung, K., López-Vidriero, I., Franco-Zorrilla, J.M., Solano, R., Trevisan, M., Pradervand, S., et al. (2012). Phytochrome interacting factors 4 and 5 control seedling growth in changing light conditions by directly controlling auxin signaling. Plant J. *71*, 699–711.
6. Hersch, M., Lorrain, S., de Wit, M., Trevisan, M., Ljung, K., Bergmann, S., and Fankhauser, C. (2014). Light intensity modulates the regulatory network of the shade avoidance response in Arabidopsis. Proc. Natl. Acad. Sci. USA *111*, 6515–6520.
7. Julkowska, M.M., and Testerink, C. (2015). Tuning plant signaling and growth to survive salt. Trends Plant Sci. *20*, 586–594.
8. Claeys, H., Van Landeghem, S., Dubois, M., Maleux, K., and Inzé, D. (2014). What Is Stress? Dose-Response Effects in Commonly Used in Vitro Stress Assays. Plant Physiol. *165*, 519–527.
9. Jiang, C., Belfield, E.J., Mithani, A., Visscher, A., Ragoussis, J., Mott, R., Smith, J.A., and Harberd, N.P. (2012). ROS-mediated vascular homeostatic control of root-to-shoot soil Na delivery in Arabidopsis. EMBO J. *31*, 4359–4370.
10. Jiang, C., Belfield, E.J., Cao, Y., Smith, J.A., and Harberd, N.P. (2013). An Arabidopsis soil-salinity-tolerance mutation confers ethylene-mediated enhancement of sodium/potassium homeostasis. Plant Cell *25*, 3535–3552.
11. Zhu, J.K. (2016). Abiotic Stress Signaling and Responses in Plants. Cell *167*, 313–324.
12. Song, L., Huang, S.C., Wise, A., Castanon, R., Nery, J.R., Chen, H., Watanabe, M., Thomas, J., Bar-Joseph, Z., and Ecker, J.R. (2016). A transcription factor hierarchy defines an environmental stress response network. Science *354*, aag1550.
13. Yoshida, T., Fujita, Y., Maruyama, K., Mogami, J., Todaka, D., Shinozaki, K., and Yamaguchi-Shinozaki, K. (2015). Four Arabidopsis AREB/ABF transcription factors function predominantly in gene expression downstream of SnRK2 kinases in abscisic acid signalling in response to osmotic stress. Plant Cell Environ. *38*, 35–49.
14. Park, S.Y., Fung, P., Nishimura, N., Jensen, D.R., Fujii, H., Zhao, Y., Lumba, S., Santiago, J., Rodrigues, A., Chow, T.F., et al. (2009). Abscisic acid inhibits type 2C protein phosphatases via the PYR/PYL family of START proteins. Science *324*, 1068–1071.

15. Fujii, H., Verslues, P.E., and Zhu, J.-K. (2007). Identification of two protein kinases required for abscisic acid regulation of seed germination, root growth, and gene expression in Arabidopsis. Plant Cell *19*, 485–494.
16. de Wit, M., Keuskamp, D.H., Bongers, F.J., Hornitschek, P., Gommers, C.M.M., Reinen, E., Martínez-Cerón, C., Fankhauser, C., and Pierik, R. (2016). Integration of Phytochrome and Cryptochrome Signals Determines Plant Growth during Competition for Light. Curr. Biol. *26*, 3320–3326.
17. Li, L., Zhang, Q., Pedmale, U.V., Nito, K., Fu, W., Lin, L., Hazen, S.P., and Chory, J. (2014). PIL1 participates in a negative feedback loop that regulates its own gene expression in response to shade. Mol. Plant *7*, 1582–1585.
18. Pfeiffer, A., Shi, H., Tepperman, J.M., Zhang, Y., and Quail, P.H. (2014). Combinatorial complexity in a transcriptionally centered signaling hub in Arabidopsis. Mol. Plant *7*, 1598–1618.
19. Liao, C.Y., Smet, W., Brunoud, G., Yoshida, S., Vernoux, T., and Weijers, D. (2015). Reporters for sensitive and quantitative measurement of auxin response. Nat. Methods *12*, 207–210, 2, 210.
20. Korver, R.A., Koevoets, I.T., and Testerink, C. (2018). Out of Shape During Stress: A Key Role for Auxin. Trends Plant Sci. *23*, 783–793.
21. Hayes, S., Velanis, C.N., Jenkins, G.I., and Franklin, K.A. (2014). UV-B detected by the UVR8 photoreceptor antagonizes auxin signaling and plant shade avoidance. Proc. Natl. Acad. Sci. USA *111*, 11894–11899.
22. Feng, S., Martinez, C., Gusmaroli, G., Wang, Y., Zhou, J., Wang, F., Chen, L., Yu, L., Iglesias-Pedraz, J.M., Kircher, S., et al. (2008). Coordinated regulation of Arabidopsis thaliana development by light and gibberellins. Nature *451*, 475–479.
23. de Lucas, M., Davière, J.M., Rodríguez-Falcón, M., Pontin, M., Iglesias-Pedraz, J.M., Lorrain, S., Fankhauser, C., Blázquez, M.A., Titarenko, E., and Prat, S. (2008). A molecular framework for light and gibberellin control of cell elongation. Nature *451*, 480–484.
24. Achard, P., Cheng, H., De Grauwe, L., Decat, J., Schoutteten, H., Moritz, T., Van Der Straeten, D., Peng, J., and Harberd, N.P. (2006). Integration of plant responses to environmentally activated phytohormonal signals. Science *311*, 91–94.
25. Djakovic-Petrovic, T., de Wit, M., Voesenek, L.A., and Pierik, R. (2007). DELLA protein function in growth responses to canopy signals. Plant J. *51*, 117–126.
26. Geng, Y., Wu, R., Wee, C.W., Xie, F., Wei, X., Chan, P.M., Tham, C., Duan, L., and Dinneny, J.R. (2013). A spatio-temporal understanding of growth regulation during the salt stress response in Arabidopsis. Plant Cell *25*, 2132–2154.
27. Yin, Y., Wang, Z.Y., Mora-Garcia, S., Li, J., Yoshida, S., Asami, T., and Chory, J. (2002). BES1 accumulates in the nucleus in response to brassinosteroids to regulate gene expression and promote stem elongation. Cell *109*, 181–191.
28. Martínez, C., Espinosa-Ruíz, A., de Lucas, M., Bernardo-García, S., Franco-Zorrilla, J.M., and Prat, S. (2018). PIF4-induced BR synthesis is critical to diurnal and thermomorphogenic growth. EMBO J. *37*, 99552.
29. Bernardo-García, S., de Lucas, M., Martínez, C., Espinosa-Ruiz, A., Davière, J.M., and Prat, S. (2014). BR-dependent phosphorylation modulates PIF4 transcriptional activity and shapes diurnal hypocotyl growth. Genes Dev. *28*, 1681–1694.
30. Zhang, S., Cai, Z., and Wang, X. (2009). The primary signaling outputs of brassinosteroids are regulated by abscisic acid signaling. Proc. Natl. Acad. Sci. USA *106*, 4543–4548.
31. Tang, W., Kim, T.W., Oses-Prieto, J.A., Sun, Y., Deng, Z., Zhu, S., Wang, R., Burlingame, A.L., and Wang, Z.Y. (2008). BSKs mediate signal transduction from the receptor kinase BRI1 in Arabidopsis. Science *321*, 557–560.
32. Kim, T.W., Guan, S., Sun, Y., Deng, Z., Tang, W., Shang, J.-X., Sun, Y., Burlingame, A.L., and Wang, Z.Y. (2009). Brassinosteroid signal transduction from cell-surface receptor kinases to nuclear transcription factors. Nat. Cell Biol. *11*, 1254–1260.
33. Sreeramulu, S., Mostizky, Y., Sunitha, S., Shani, E., Nahum, H., Salomon, D., Hayun, L.B., Gruetter, C., Rauh, D., Ori, N., and Sessa, G. (2013). BSKs are partially redundant positive regulators of brassinosteroid signaling in Arabidopsis. Plant J. *74*, 905–919.
34. Li, Z.Y., Xu, Z.S., He, G.Y., Yang, G.X., Chen, M., Li, L.C., and Ma, Y.Z. (2012). A mutation in Arabidopsis *BSK5* encoding a brassinosteroid-signaling kinase protein affects responses to salinity and abscisic acid. Biochem. Biophys. Res. Commun. *426*, 522–527.
35. Kohnen, M.V., Schmid-Siegert, E., Trevisan, M., Petrolati, L.A., Sénéchal, F., Müller-Moulé, P., Maloof, J., Xenarios, I., and Fankhauser, C. (2016). Neighbor Detection Induces Organ-Specific Transcriptomes, Revealing Patterns Underlying Hypocotyl-Specific Growth. Plant Cell *28*, 2889–2904.
36. Yu, X., Li, L., Zola, J., Aluru, M., Ye, H., Foudree, A., Guo, H., Anderson, S., Aluru, S., Liu, P., et al. (2011). A brassinosteroid transcriptional network revealed by genome-wide identification of BESI target genes in Arabidopsis thaliana. Plant J. *65*, 634–646.
37. Oh, E., Zhu, J.Y.J., Bai, M.Y., Arenhart, R.A., Sun, Y., and Wang, Z.Y. (2014). Cell elongation is regulated through a central circuit of interacting transcription factors in the Arabidopsis hypocotyl. eLife *3*, 1–19.
38. Oh, E., Zhu, J.Y., and Wang, Z.Y. (2012). Interaction between BZR1 and PIF4 integrates brassinosteroid and environmental responses. Nat. Cell Biol. *14*, 802–809.
39. Ling, J.J., Li, J., Zhu, D., and Deng, X.W. (2017). Noncanonical role of *Arabidopsis* COP1/SPA complex in repressing BIN2-mediated PIF3 phosphorylation and degradation in darkness. Proc. Natl. Acad. Sci. USA *114*, 3539–3544.
40. Sakuraba, Y., Bülbül, S., Piao, W., Choi, G., and Paek, N.C. (2017). Arabidopsis EARLY FLOWERING3 increases salt tolerance by suppressing salt stress response pathways. Plant J. *92*, 1106–1120.
41. Kahlaoui, B., Misle, E., Khaskhoussy, K., Jaouadi, I., and Hachicha, M. (2016). Brassinosteroids and drought tolerance in plants. In Water Stress and Crop Plants: A Sustainable Approach, P. Ahmad, ed. (Wiley), pp. 600–607.
42. Davis, A.M., Hall, A., Millar, A.J., Darrah, C., and Davis, S.J. (2009). Protocol: Streamlined sub-protocols for floral-dip transformation and selection of transformants in Arabidopsis thaliana. Plant Methods *5*, 3.

STAR★METHODS

KEY RESOURCES TABLE

REAGENT or RESOURCE	SOURCE	IDENTIFIER
Antibodies		
High Affinity Anti-HA-HRP (3F10)	Roche	RRID:AB_390914
Anti-GFP-HRP	Miltenyi Biotec	RRID:AB_2470
Bacterial Strains		
E.coli (DH5α)	N/A	N/A
A. tumefaciens (AGL1)	N/A	N/A
Chemicals, Peptides and Recombinant Proteins		
Murashige &Skoog (MS) medium	Duchefa Biochemie	M0222.0050
Silwet® L-77	Phytotech Labs	S7777
Epibrassinolide	Santa-Cruz Biotechnology	sc-211419
Abscisic Acid	Sigma Aldrich	862169
Brassinazole	Sigma Aldrich	SML1406
Luciferin	Promega	E1601
X-glucuronide	Sigma Aldrich	B5285-10MG
SuperSignal West Femto	Thermo Fisher Scientific	34095
SuperSignal West Pico PLUS	Thermo Fisher Scientific	34580
FastDigest SacI	Thermo Fisher Scientific	FD1133
FastDigest NotI	Thermo Fisher Scientific	FD0593
FastDigest EcoRI	Thermo Fisher Scientific	FD0274
FastDigest BamHI	Thermo Fisher Scientific	FD0054
FastDigest Green Buffer (10X)	Thermo Fisher Scientific	B72
Critical Commercial Assays		
RNeasy Mini Kit	QIAGEN	74106
RNase-Free DNase Set (50)	QIAGEN	79254
QIAprep Spin Miniprep Kit	QIAGEN	27106
Nucleospin Gel and PCR Clean-up	Macherey-Nagel	740609
RevertAid First Strand cDNA Synthesis Kit	Thermo Fisher Scientific	K1621
SsoAdvanced Universal SYBR Green Supermix	Bio-Rad	1725271
Deposited Data		
PIF4/5-HA western blots	https://zenodo.org/record/1343501#.XH_f2ohKg2w	N/A
BES1-GFP western blots	https://zenodo.org/record/1480822#.XH_fCohKg2w	N/A
GUS staining images	https://zenodo.org/record/2022607#.XH_f74hKg2w	N/A
Raw data for figure generation	https://zenodo.org/record/2592526#.XIk36yhKg2w	N/A
Experimental Organisms		
Col-0	N/A	N/A
Ws	N/A	N/A
Ler	N/A	N/A
pif4-101	3	Garlic_114_G06
pif5 (pil6-1)	43	SALK_087012
pif7-1	44	SALK_044061
pif4-101/pif5 (aka *pil6-1*)	3	Garlic_114_G06/ SALK_087012

(*Continued on next page*)

Continued		
REAGENT or RESOURCE	SOURCE	IDENTIFIER
pif4-101/pif5 (aka *pil6-1*)/ *pif7-1*	45	Garlic_114_G06/ SALK_087012/ SALK_044061
abaQ (*pyr1-1/pyl1-1/pyl2-1/pyl4-1*)	14	Point/ Salk_054640/ CSHL_GT2864_1/ Sail_517_C08
snrk2.2/snrk2.3	15	GABI_807G04/ Salk_107315
arebQ (*areb1/ areb2/ abf3/ abf1-1*)	13	SALK_002984/ SALK_069523/ SALK_096965/ SALK_132819
abi5-1	46	N/A
bes1-D	27	N/A
gsk3-triple (*bin2-3bil1-1bil2-1*)	47	FLAG_593C09/Wisonsin KO /Wisonsin KO
bsk5	NASC (characterized in 34)	SALK_051739C
aba2-1	48	N/A
aba3-1	48	N/A
della global (*gai-t6/ rga-t2/ rgl1-1/ rgl2-1/ rgl3-4*)	49	N/A
pPIL1:LUC	17	N/A
pIAA19:LUC	New line	N/A
pDR5V2:GUS	New line	N/A
pDR5V2:GUS/ pif4-101/ pif5 (pil6-1)	New line	N/A /Garlic_114_G06/ SALK_087012
p35S:PIF4-HA	Franklin Lab, Bristol, UK	N/A
p35S:PIF5-HA	Franklin Lab, Bristol, UK	N/A
p35S:BES1-GFP	28	N/A
Tomato- S.lycopersicum var. "Moneymaker"	Intratuin, NL	EAN# 8717263349600
Tobacco- N. benthamiana	N/A	N/A
Recombinant DNA		
pENTR_D-TOPO	Thermo Fisher	K2400-20
LucTrap3	N/A	GenBank: AY968054.1
pGREENII0179	N/A	N/A
pUC57:DR5v2	Dolf Weijers (WUR)	N/A
Software and Algorithms		
Microsoft Excel 2010	Microsoft	N/A
Microsoft Powerpoint 2010	Microsoft	N/A
Microsoft Word 2010	Microsoft	N/A
SPSS Statistics 24	IBM	N/A
Snapgene	GSL Biotech LLC	N/A
ImageJ	NIH	N/A
ICY	Quantitative Image Analysis Unit, Institut Pasteur	N/A
GIMP2	The GIMP Development Team	N/A
ViiA 7 Software	Thermo Fisher Scientific	N/A
Prism 6	Graphpad	N/A

CONTACT FOR REAGENT AND RESOURCE SHARING

Further information and requests for resources and reagents should be directed to and will be fulfilled by the Lead Contact, Ronald Pierik (r.pierik@uu.nl).

EXPERIMENTAL MODEL AND SUBJECT DETAILS

The main experimental organism used in this study was *Arabidopsis thaliana*. Several mutant *Arabidopsis* lines were used: *pif4-101*, *pif5* (*pil6-1*), *pif7-1*, *pif4-101/pif5* (*pil6-1*), *pif4-101/pif5* (*pil6-1*)/ *pif7-1*, *abaQ* (*pyr1-1/pyl1-1/pyl2-1/pyl4-1*), *snrk2.2/snrk2.3*, *arebQ* (*areb1/ areb2/ abf3/ abf1-1*), *bsk5*, *aba2-1*, *aba3-1*, *pPIL1:LUC* and *p35S:BES1-GFP* in the Columbia ecotype; *abi5-1* and *gsk3-triple*

(*bin2-3/bil1-1/bil2-1*) in the Ws ecotype; and *della global* (*gai-t6/ rga-t2/ rgl1-1/ rgl2-1/ rgl3-4*), *p35S:PIF4-HA* and *p35S:PIF5-HA* in the L*er* ecotype. The other species used in this study were tomato (*S.lycopersicum* var. "Moneymaker") and tobacco (*N. benthamiana*). See the Key Resources Table for details.

PLANT PROPAGATION

To generate the seed used in this study, plants were grown in 130-140 μmol m^{-2} s^{-1} white light with a 16h 8h photoperiod at 21°C. Plants were kept well-watered until silique senescence, after which water was increasingly withheld until the plant was fully senesced. Harvested seeds were stored dry at room temperature for at least 2 weeks before use.

METHOD DETAILS

Morphological studies

Seeds were sown directly onto wetted soil and stratified at 4°C in darkness. After 3-4 days of stratification, plants were moved to growth chambers with a 16:8 hour photoperiod (PP), 130-140 μmol m^{-2} s^{-1} white light at 21°C. After 3 days, plants were transferred to new soil that had been previously wetted with deionised water or the indicated concentration of NaCl and then returned to white light for the indicated period. WI +FR treatments were provided by supplementary FR LEDs to a R:FR ratio of 0.2.

Development of Transgenic Lines

pDR5v2:GUS- The *pGREENII0179:pDR5v2:GUS* plasmid was constructed by ligating a *pDR5v2* fragment cut from *pUC57:DR5v2* [19] with EcoRI and BamHI into *pGREENII0179* lacking a promoter. The *GUS* gene was amplified from a *pDR5:GUS Arabidopsis* line containing a *GUS* reporter with primers introducing NotI and SacI restriction sites. The PCR fragment was subsequently cut with NotI and SacI and ligated into *pGREENII0179:pDR5v2* to create *pGREENII0179:pDR5v2:GUS*. This was then transformed into *E.coli* (strain- DH5α) and sequenced to confirm the correct insertion of *GUS*. The *pDR5v2:GUS Arabidopsis* line was made transforming *pGREENII0179:pDR5v2:GUS* into *agrobacterium* (strain AGL1) containing the *pSOUP* plasmid. This was then transformed into Col-0 plants by floral dipping, as in reference [42]. Briefly, agrobacterium were grown in YEBS media to saturation, and Silwet® L-77 was added to 200ul/l. *Arabidopsis* inflorescence stems were dipped into the solution and seeds harvested after senescence. 21 independent transformants were selected by antibiotic resistance and T2 lines screened for single insertions and GUS staining intensity. T3 homozygous lines were selected by hygromycin resistance and checked for signal strength, distribution and auxin responsiveness.

pIAA19:LUC- The *pIAA19:LUC* plasmid was constructed by amplifying the *IAA19* promoter from *Arabidopsis thaliana* (Col ecotype), with the primers listed in the key resources table (see online). The promoter fragment was then cloned into *pENTR_D-TOPO* and mobilized into the LucTrap3 vector. This construct was then transformed into *agrobacterium* (strain AGL1) and used for transformation of Col-0 plants by floral dip as above.

p35S:PIF4-HA and *p35:PIF5-HA*- The *pCF402* and *pCF404* plasmids (described previously in [3]) were introduced into *agrobacterium* and then transformed into L*er* plants by floral dip. Transformed lines were selected based on seed-coat GFP fluorescence. These lines are very similar to existing lines in the Col-0 background [3].

For oligonucleotides used in this study see STAR Methods.

Gene Expression Studies

Seedlings were grown in the indicated conditions, before dissection and flash freezing in liquid nitrogen. RNA was extracted with an RNeasy Mini Kit (QIAGEN) with an on-column treatment with DNase (QIAGEN). cDNA was synthesized using a RevertAid First Strand cDNA Synthesis Kit (Thermo Fisher Scientific) with random hexamers. qPCR was performed with SYBR green ready mix (Bio-rad) in a ViiA 7 Real-Time PCR System (Thermo Fisher Scientific). Ct values for the gene of interest are expressed relative to that Ct value found for primers targeted to *AT1G13320*. For each experiment, 2 technical and a minimum of 3 biological repeats was performed. Primer efficiency tests were performed for each primer pair used.

For oligonucleotides used in this study see STAR Methods.

Luciferase Assay

pPIL1:LUC and *pIAA19:LUC* seedlings were germinated in 1/2 MS media at 120-140 μmol$m^{-2}s^{-1}$ white light (16h:8h PP) at 22°C. On cotyledon expansion, seedlings were transferred to microtiter plates containing 170 μl solid 1/2 MS media (6% agar) supplemented with EtOH (mock), 75 mM NaCl (NaCl), or 2 μM ABA, per well. 30 μl of a luciferin solution (8 μl of a 10 mg/ ml luciferin (Promega) stock in DMSO, diluted in 4 mL H2O) were added per well, and plates were sealed with a sealing film (Applied Biosystems). Two holes were then made with a fine needle per well for seedlings transpiration. Plants were moved to red light (30-35 μmol m^{-2} s^{-1}-16h:8h PP) and luminescence was recorded by a Berthold LB960 station installed in a Percival growth chamber. Luminescence was recorded each hour, with a 2 s read per well. On day 2 at Zt4, R light was supplemented with FR.

ABA Extraction and Quantification

Plants were grown under the same conditions used for morphological studies. At Zt 4 on day 7, 20-50mg of tissue (approximately 50 seedlings) were harvested and flash frozen in liquid nitrogen. Samples were homogenized (Precellys 24, Bertin Technologies, Aix-en-Provence, France) and extracted in ethyl acetate with an internal standard of D6-ABA (C/D/N Isotopes Inc, Canada). Samples were dried on a vacuum concentrator (CentriVap Centrifugal Concentrator, Labconco, Kansas City, MO, USA) at room temperature. Residues were re-suspended in 0.25 mL of 70% methanol (v/v) and samples were analyzed by liquid chromatography-mass spectrometry (LC-MS) on a Varian 320 Triple Quad LC-MS/MS. ABA levels were quantified from the peak area of each sample compared with the internal standard and normalized by fresh weight.

Western Blots

Plants were germinated on 1/2 MS plates in white light (120-140 μmol m^{-2} s^{-1} −16:8h PP) for 3 days at 21°C, before being transferred to plates with or without 75mM NaCl. Plates were then grown in R light (30-35 μmol m^{-2} s^{-1} −16:8h PP) for a further 2 days. On day 5, at Zt 3, half the plates were moved to R+FR light. Tissues were harvested at Zt 4. 10 seedlings were homogenized and proteins were extracted in 70 μl Cracking Buffer (125mM Tris pH 7.4, 2% SDS, 10% Glycerol, 6M Urea, 5% βME) and 15 μl of the extract was run on a 10% polyacrylamide gel. Blots were probed with anti-HA-HRP (Roche) or anti-GFP-HRP (Miltenyi Biotec) as indicated in the text. Membranes were developed with 50/50 mix of 'pico' and 'femto' chemiluminescence substrates (Thermo) on a ChemiDoc (Biorad).

GUS Staining

Tissues were harvested an immediately fixed in 90% acetone at −20°C. Tissues were washed twice under a vacuum in GUS wash solution (0.1M Phospho-PI pH 7.0, 10 mM EDTA, 2 mM $K_3Fe(CN)_6$) and then stained overnight at 37°C in GUS staining solution (0.1M Phospho-PI pH 7.0, 10 mM EDTA, 1 mM $K_3Fe(CN)_6$, 1mM $K_4Fe(CN)_6$ * $3H_2O$, 0.5 mg/ ml X-glucuronide). The GUS reaction was stopped by treatment with 3:1 ethanol: acetic acid mix for 1 hour at 37°C. Tissues were cleared with 70% ethanol over several days and then mounted in 10% chloral hydrate, 30% glycerol. Representative images were taken with a Zeiss Axioskop 2 with Infinity 3 camera attachment and slides were scanned with an Epson v300 scanner for the purposes of GUS quantification.

QUANTIFICATION AND STATISTICAL ANALYSES

Image quantification

For morphological studies, plants were laid out on 0.8% agar plates and scanned with an Epson v300 scanner. Length measurements were then made in ImageJ. Western blot band intensities were quantified by measuring pixel intensity in ImageJ. Total protein loading was assessed through Rubisco Large Subunit band intensity, as visualized through ponceau stinging. Total protein loading was then used to normalize chemiluminescence blot band intensity. GUS staining quantification was performed in the ImageJ-based program, Icy. Relative GUS levels in the top half of the hypocotyl were defined by the mean intensity in Ch-0 minus the mean intensity in Ch-1.

Data presentation

Data presented as box and whisker diagrams were created in Graphpad Prism, and compiled in Microsoft Powerpoint. Datasets where $n \geq 10$ are represented with a Tukey representation. The upper and lower edges of the box represent interquartile range (IQR) and the middle bar represents the median value. values 1.5 x IQR higher than the 75th percentile or 1.5x IQR lower than the 25th percentile are marked as single point outliers. Whiskers are plotted as the maximum and minimum values, or as 1.5x IQR, depending on which is closer to the median. Datasets where $n \leq 10$ are presented as box and whisker diagrams, with all points shown. Whiskers represent the maximum and minimum values.

Statistical Analyses

1-way and 2-way ANOVAs were performed in Graphpad Prism or with SPSS statistics. t tests were performed in Microsoft Excel. Significant differences are defined as $p > 0.05$. In graphs that include letters, each letter represents a statistically significant mean.

DATA AVAILABILITY

The data used in the preparation of this manuscript, including morphological measurements, average Ct values, image analyses, ABA quantifications and photon counts is available at the following site: https://zenodo.org/record/2592526#.XIk36yhKg2w

The images used for western blot quantification are available at the sites listed below:

PIF4-HA and PIF5-HA: https://zenodo.org/record/1343501#.XH_f2ohKg2w
BES1-GFP: https://zenodo.org/record/1480822#.XH_fCohKg2w

The images used for GUS-staining quantification are available at the site listed below:

DR5v2:GUS in both Col and *pif4pif5* mutants: https://zenodo.org/record/2022607#.XH_f74hKg2w